Int. J. Heat Mass Transfer. Vol. 13, pp. 932–937. Pergamon Press 1970. Printed in Great Britain

AN EXPERIMENTAL STUDY OF MIXING PHENOMENA OF TURBULENT SUPERSONIC JETS

J. D. KAPNER,* KUN LI and R. H. LARSON

Department of Chemical Engineering, Carnegie-Mellon University, Pittsburgh, Pennsylvania 15213

(*Received* 3 *September* 1968 *and in revised form* 29 *April* 1969)

NOMENCLATURE

D, diameter;
M, local Mach number, u/c;
m, mass flow rate;
p, pressure;
r, radius;
T, time-averaged temperature;
u, time-averaged velocity in axial direction;
x, axial coordinate;
y, radial coordinate;
σ, turbulent Prandtl number;
ρ, fluid density.

Subscripts
e, condition at nozzle exit;
m, condition at jet axis;
0, initial condition or characteristic value (as x_0);
p, temperature probe reading;
s, condition of surroundings;
x, any axial position;
$\frac{1}{2}$, radial position where $u/u_m = \frac{1}{2}$.

INTRODUCTION

IN RECENT years, the use of supersonic oxygen jets in the basic oxygen steelmaking process, which has become increasingly important, has stimulated interest in the problem of compressible turbulent jets exhausting into hot reactive surroundings. A review of the literature shows relatively little work for the case of cold jets exhausting into hot surroundings and practically no work on the corresponding reactive situation. This work was initiated to provide basic information for a better understanding of the mixing phenomena in such a system. The present paper reports some experimental data obtained for an axisymmetrical supersonic air jet exhausting into a hot medium of air, and a comparison of the experimental results with the theoretical analysis of Laufer [8]. The variables studied were the Mach number of the jet and the initial temperature difference between the jet and surroundings.

EXPERIMENTAL METHODS

The apparatus consisted of a test section enclosed by an insulated 2 ft diameter by 3 ft high steel drum with a conical shaped entrance for the surrounding air. A test nozzle directed vertically downward was located at the center. Compressed air supplied to the nozzle was dehumidified, filtered and metered. Two surge tanks were used to eliminate the pulsation of the compressor and a diaphram pressure regulator to control the nozzle upstream pressure. The surrounding air was provided by a rotary blower. Both the jet and surrounding air systems were equipped with resistance heaters.

To limit the entrainment of the surrounding air by the jet within the region of interest, the expanding jet was exhausted from the test section through a 3 in. diameter opening in a movable baffle. All the measurements were made at points above the baffle. The opening in the baffle was large enough so that the flow characteristics being measured were not altered. This was verified by two otherwise identical runs at Mach 1·8 with and without the baffle which showed no more differences than any other set of duplicate runs.

All measurements were taken at steady state after careful alignment of the Pitot tube or total temperature probe. The Pitot tube was a 22 gauge (0·023 in. o.d.) hypodermic needle, $\frac{3}{4}$ in. long with a slightly conical tip and a sharp lip. The total temperature probe was of the diffuser type, 0·042 in. o.d. with an iron–constantan grounded junction thermocouple. The probe was positioned by means of a traverse mechanism capable of positioning the probe to within 0·001 in. vertically or horizontally. The pressure or temperature measurements were taken separately.

The test nozzles used were designed on the basis of isentropic flow and all had a total convergent angle of 30°. The three nozzles used had nominal Mach numbers of 1·0 (0·08875 in. diameter), 1·4 (0·0841 in. throat diameter and 10° total divergence angle) and 1·8 (0·0595 in. throat diameter and an 18° total divergence angle).

* Present address: E. I. du Pont de Nemours & Company, Electrochemicals Department, Nigara Falls, New York 14302.

From the measured dynamic pressures, the local Mach number and velocity field were calculated using the Pitot tube formulas with the assumption of the ideal gas law and the static pressure being equal to the ambient pressure. When the effect of a shock wave in front of the Pitot tube becomes significant (above Mach 1·3), the presence of the shock wave was accounted for by the Rayleigh–Pitot tube formula. The temperature probe was calibrated in the exit plane of several nozzles where the stagnation temperature was known by assuming isentropic flow through the nozzle, yielding the following relationship,

$$\frac{T}{T_P} = [1 + 0{\cdot}1855\mathrm{M}^{1{\cdot}95}]^{-1} \tag{1}$$

which was used to calculate the stream temperature from the measured total temperatures.

In the pilot tube measurements of dynamic pressure, the estimated accuracy is $\pm 0{\cdot}1$ in. H_2O in the range 0–30 in. H_2O, $\pm 1{\cdot}0$ mmHg in the range 30–900 mmHg, and $\pm 0{\cdot}1$ psi in the range 15–70 psig. The standard error as given by the supplier for the thermocouples is $+4°F$ in the range 0–530°F. Nozzle flow measured by a rotameter is estimated to be within $+1$ per cent.

An indication of the reliability of the experimental results can be obtained by a momentum balance. Assuming the static pressure equal to the ambient pressure, the total momentum in the axial direction is conserved at any cross section. The values of momentum computed at various cross sections were found to deviate from the value at the exit by less than 5 per cent for most runs, and in general less than 10 per cent.

RESULTS AND DISCUSSION

Presentation of data

The axial decays of velocity and temperature are presented for all the runs of Mach 1·0, 1·4 and 1·8 in Figs. 1 and 2 with experimental conditions indicated. The coordinates used are consistent with the theory of Laufer [8] to be discussed later. In general, the axial decay of velocity decreases as the Mach number or the temperature difference between the surroundings and the jet increases. Similar behavior is observed for the axial temperature decay.

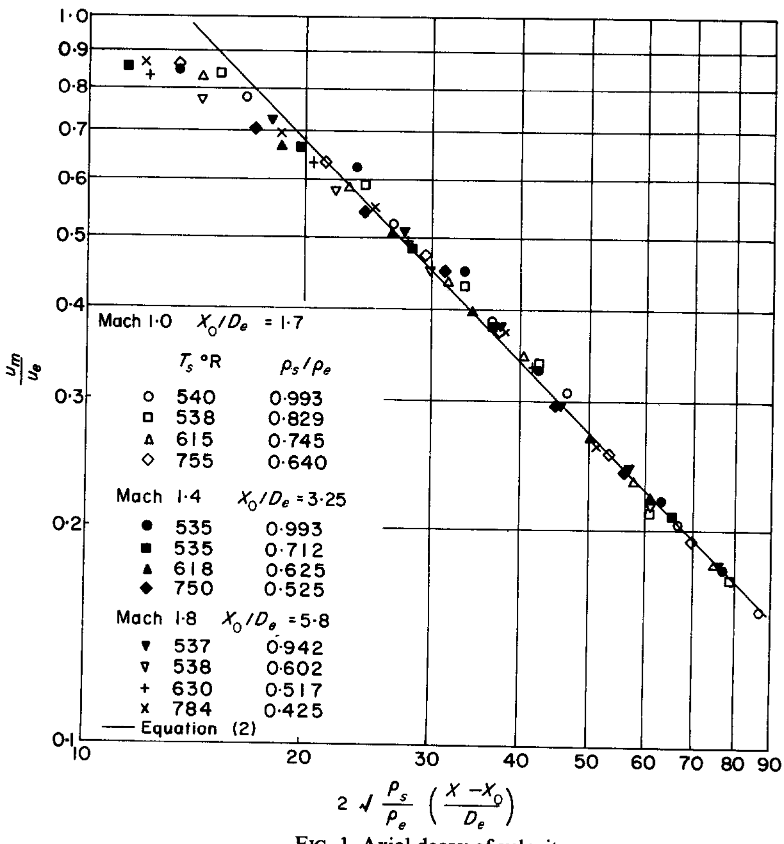

FIG. 1. Axial decay of velocity.

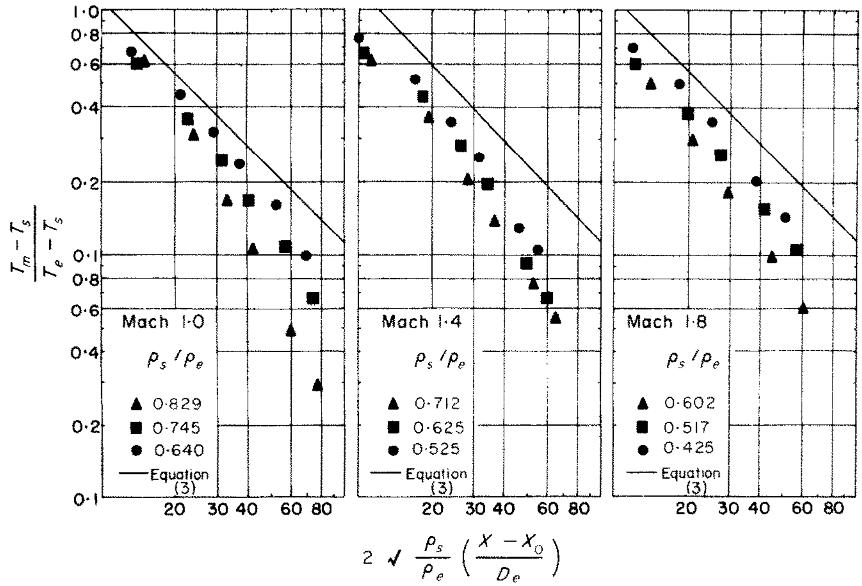

FIG. 2. Axial decay of temperature.

Comparison of the decay curves shows that temperature decays faster than velocity.

Figure 3 shows the extent of jet spreading as represented by the half radius ($r_{\frac{1}{2}}$) which is defined as the radial distance where the velocity is one half the velocity at the axis. For clarity, only the data from the runs of the highest and lowest temperature differences are included. The coordinates were so chosen that the data can be conveniently compared with theory.

The radial distribution of velocity is presented in Figs. 4 and 5. It is seen in Fig. 4 that as x/D_e increases, the profiles gradually converge to a single curve. The axial distance where the profile becomes similar can be taken to mark the beginning of the fully developed region. This occurs at $x/D_e = 15$ for Mach 1·0, $x/D_e = 25$ for Mach 1·4 and $x/D_e = 35$ for Mach 1·8. Representative points in the fully developed region for all Mach numbers are plotted in Fig. 5.

Due to scatter in the temperature data, only a composite profile in the developed region is shown in Fig. 5. Generally, a greater degree of scatter occurs at large axial distances where temperature fluctuations were large compared to $(T_s - T_m)$. This was noted when $(T_s - T_m)$ became less than 10–15°F.

A comparison of the velocity and temperature profiles in Fig. 5 confirm the observation that the turbulent transport of heat is faster than momentum. As a by product, the entrainment defined as $(m_x - m_o)/m_o$ was calculated from the velocity and temperature data and presented in Fig. 6.

The present data on axial decay of velocity were found to be in good agreement with the data of Fenn [5] for Mach 1·0, Warren [12] Mach 0·97, Voorheis [11] Mach 0·96 and

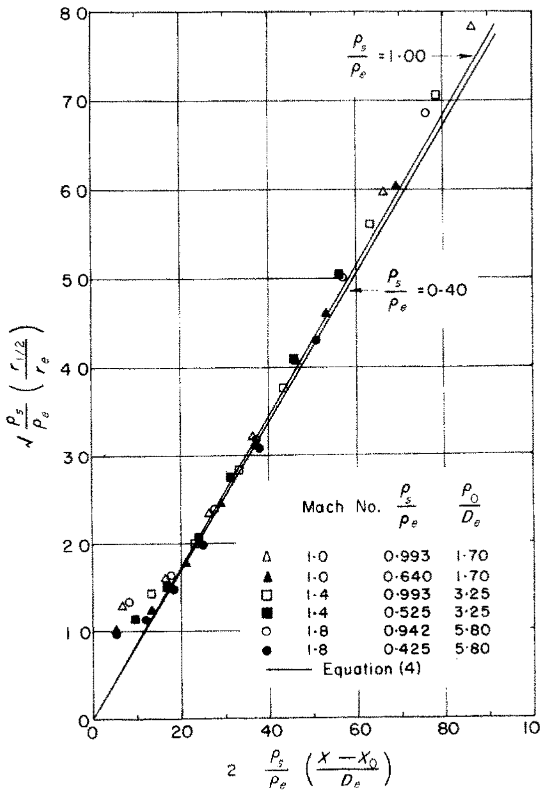

FIG. 3. Jet spreading.

Johannesen [6] Mach 1·4 under comparable experimental conditions. The composite radial distributions of velocity and temperature in the developed region reported by Anderson and Johns [2] for Mach 1·4 and 1·84 hot air jets with initial stagnation temperatures from 1200 to 1960°R exhausting into quiescent atmosphere are included in Fig. 5. It can be seen that their profiles follow closely those of this work.

Comparison with theory

Most of the theoretical analyses [1, 3, 7, 10, 12] of compressible, turbulent jets have been based on the assumption that eddy viscosity or turbulent transfer coefficient is only a function of the axial coordinate. A wide variety of expressions for eddy viscosity has been proposed by various authors. Recently, Eggers [4] computed the eddy viscosity

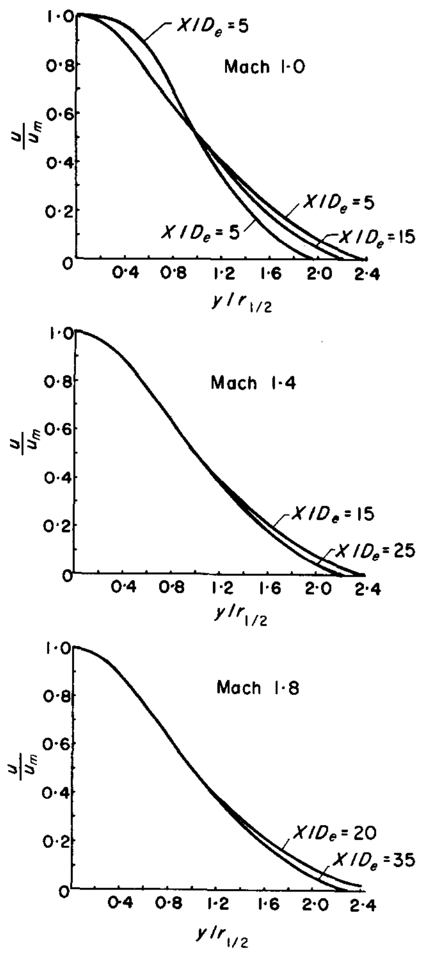

FIG. 4. Radial distribution of velocity.

distributions from his experimental data on a Mach 2·22 jet and concluded that the assumption of eddy viscosity being independent of the radial coordinate is not justified.

In a different approach, Laufer [8] transformed the compressible momentum and energy equations into the incompressible form by the method of coordinate stretching. Thus, if the velocity field in an incompressible flow is known, the corresponding compressible case can be calculated without assuming an explicit form for a compressible turbulent exchange coefficient. By invoking a similarity hypothesis concerning the turbulent momentum and heat transfer in the fully developed region, Laufer obtained the following expressions for the axial decays of velocity and temperature, and for the axial variation of the half radius

$$\frac{u_m}{u_e} = 13{\cdot}6\left[2\left(\frac{\rho_s}{\rho_e}\right)^{\frac{1}{2}}\frac{x - x_0}{D_e}\right]^{-1} \tag{2}$$

$$\frac{T_m - T_s}{T_e - T_s} = 6{\cdot}85(\sigma + 1)\left[2\left(\frac{\rho_s}{\rho_e}\right)^{\frac{1}{2}}\frac{x - x_0}{D_e}\right]^{-1} \tag{3}$$

$$\left(\frac{r_{\frac{1}{2}}}{r_e}\right)^2 = 0{\cdot}0294\left(\frac{x - x_0}{D_e}\right)^2 + 0{\cdot}0736\left(\frac{(\rho_s/\rho_e) - 1}{\rho_s/\rho_e}\right)\left(\frac{\rho^s}{\rho^e}\right)^{\frac{1}{2}}\left(\frac{x - x_0}{D_e}\right) \tag{4}$$

where σ is the turbulent Prandtl numer, the value of x_0 depends on the flow conditions at the nozzle exit. Because of the simplicity of these equations and difficiencies in other theoretical treatments, only a comparison of this analysis with the present data is presented.

Figure 1 shows good agreement between equation (2) and the measured centerline velocities. The values of x_0 determined from the best fit of experimental data are: x_0/D_e = 1·7 for Mach 1·0, 3·25 for Mach 1·4 and 5·8 for Mach 1·8. It is also noted that the agreement extends well beyond the fully developed region of the jet.

As shown in Fig. 2, the axial decay of temperature plotted in terms of parameters in equation (3) does not yield a single line as predicted by the theoretical analysis. Furthermore, with a value of 0·64 suggested by Laufer for the turbulent Prandtl number, the theoretical line given by equation (3) generally lies above the experimental points. The inadequacy of equation (3) may possibly be attributed to the neglect of the turbulent dissipation term in the energy equation. Also, as will be seen later, the assumption by Laufer that the radial distribution of temperature is related to that of velocity through a constant turbulent Prandtl number is not valid over the entire mixing region.

In Fig. 3, the values of the half radius calculated from equation (4) are shown for ρ_s/ρ_e = 1·0 (the isothermal case) and ρ_s/ρ_e = 0·40. This spread of density ratios covers the range of experimental data. The agreement between experimental results and equation (4) is quite satisfactory although

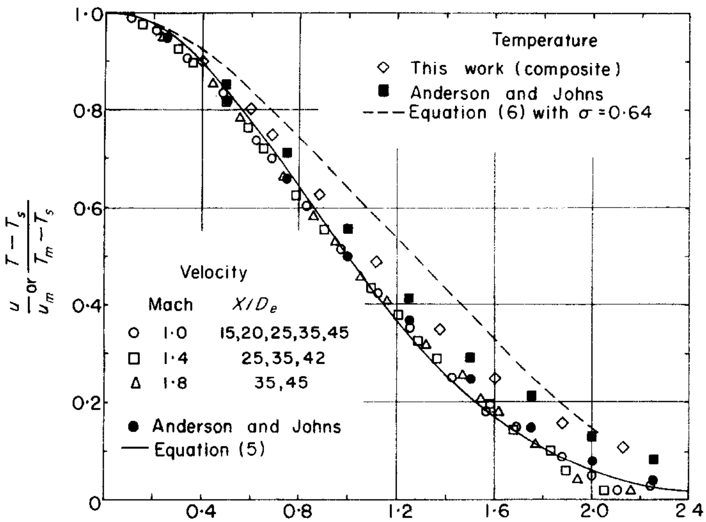

FIG. 5. Radial distribution of velocity and temperature in developed region.

the data points indicate a slightly greater slope in the linear region than the theoretical lines.

The radial distribution of velocity in the fully developed region is shown in Fig. 5 to be satisfactorily represented by the equation of Reichardt [9], a form assumed in Laufer's analysis

$$\frac{u}{u_m} = \exp\left[-\ln 2\left(\frac{y}{r_{\frac{1}{2}}}\right)^2\right]. \quad (5)$$

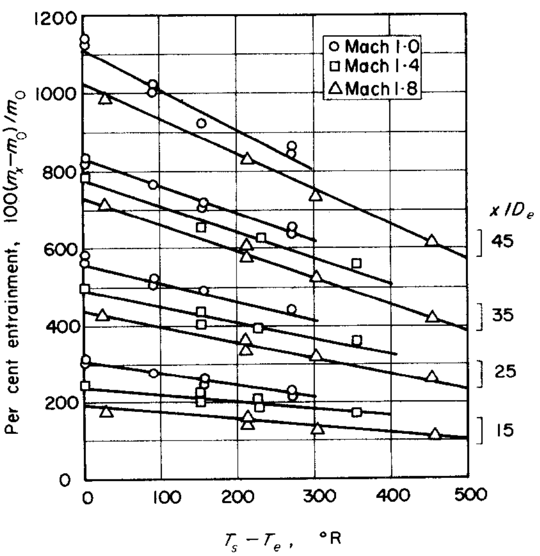

FIG. 6. Entrainment.

Laufer further assumes that the radial distribution of temperature in this region is related to the velocity distribution by

$$\frac{T - T_s}{T_m - T_s} = \left(\frac{u}{u_m}\right)^\sigma. \quad (6)$$

From the composite profiles of velocity and temperature in this work, the value of σ was found to vary between 0·82 and 0·84 within the region from the jet axis to $y/r_{\frac{1}{2}} = 1{\cdot}75$. In the outer region, it falls off to about 0·69. Equation (6) is plotted in Fig. 5 for $\sigma = 0{\cdot}64$, a value used by Laufer, for the purpose of comparison.

It may be noted that the value of σ obtained from the present data is considerably higher than 0·64. If a value of 0·83 instead of 0·64 were used in equation (3), the theoretical line for the axial temperature decay would deviate further from the experimental data.

Since no adequate theoretical analysis exists for the transition region of the jet, comparison of experiment with theory was not attempted.

CONCLUSIONS

The experimental results of this work show that the axial decay of velocity decreases as the Mach number or temperature difference between the surroundings and the jet increases. Similar behavior was found for the axial temperature decay and jet spreading. The radial distribution of velocity gradually converges to a similar profile as the axial distance increases. The axial distance where the profile becomes similar marks the beginning of the fully developed region. This occurs at $x/D_e = 15$ for Mach 1·0, $x/D_e = 25$ for

Mach 1·4, and $x/D_e = 35$ for Mach 1·8. A comparison of the velocity and temperature measurements confirms that the turbulent transport of heat is faster than momentum.

The theoretical analysis of Laufer is found to be in good agreement with the measured axial decay of velocity and jet spreading, but inadequate to account for the effects of Mach number and density differences on the axial decay of temperature. In the fully developed region, the radial distribution of velocity is satisfactorily represented by Reichardt's equation. The radial distribution of temperature can be related to that of velocity by the turbulent Prandtl number which was found to vary from 0·83 in the central region to 0·69 near the edge of the jet.

ACKNOWLEDGEMENT

The authors express their sincere appreciation to the American Iron and Steel Institute for financial support during the course of this work at Carnegie–Mellon University.

REFERENCES

1. G. N. Abramovich, *The Theory of Turbulent Jets*. M.I.T. Press, Cambridge (1963).
2. A. R. Anderson and F. R. Johns, Characteristics of free supersonic jets exhausting into quiescent air, *Jet Propulsion* **25**, No. 1, 13 (1955).
3. C. Donaldson and K. E. Gray, Theoretical and experimental investigation of the compressible free mixing of two similar gases, *AIAA Jl* **4**, (11), 2017 (1966).
4. J. M. Eggers, Velocity profiles and eddy viscosity distributions downstream of a Mach 2·22 nozzle exhausting to quiescent air, *NASA TN D*-3601 (1966).
5. R. W. Fenn, An investigation of entrainment in sonic and supersonic free air jets, M.S. thesis, Carnegie–Mellon University (1963).
6. N. H. Johannesen, Further results in the mixing of free axially-symmetrical jets of Mach number 1·4, R. & M. No. 3292, British ARC (1962).
7. G. Kleinstein, Turbulent mixing in axially symmetric free jets, *J. Spacecraft Rockets* **1**, 403 (1964).
8. John Laufer, On turbulent shear flows of variable density, Paper 68-41, presented at AIAA 6th Aerospace Sciences Meeting, New York, January 22–24 (1968).
9. H. Reichardt, On a new theory of free turbulence, *Roy. Aero. Soc.* **47**, 167 (1943); trans. from *Z.A.M.M.* **21**, 257 (1941).
10. J. F. Tomich and Eric Weger, Some new results on momentum and heat transfer in compressible turbulent free jets, *A.I.Ch.E. Jl* **13**, 948 (1967).
11. T. S. Voorheis, Entrainment of air by axially symmetric gas jets, M.S. thesis, University of California, Berkeley (1939).
12. W. R. Warren, Jr., An analytical and experimental investigation of compressible free jets, Ph.D. thesis, Princeton University (1957).